MOLECULAR BIOLOGY

Argininosuccinate synthase 1 is an intrinsic Akt repressor transactivated by p53

Takafumi Miyamoto,[1] Paulisally Hau Yi Lo,[1] Naomi Saichi,[2] Koji Ueda,[2] Makoto Hirata,[1] Chizu Tanikawa,[1] Koichi Matsuda[1,3]*

The transcription factor p53 is at the core of a built-in tumor suppression system that responds to varying degrees of stress input and is deregulated in most human cancers. Befitting its role in maintaining cellular fitness and fidelity, p53 regulates an appropriate set of target genes in response to cellular stresses. However, a comprehensive understanding of this scheme has not been accomplished. We show that *argininosuccinate synthase 1* (*ASS1*), a citrulline-aspartate ligase in de novo arginine synthesis pathway, was directly transactivated by p53 in response to genotoxic stress, resulting in the rearrangement of arginine metabolism. Furthermore, we found that x-ray irradiation promoted the systemic induction of *Ass1* and concomitantly increased plasma arginine levels in *p53*$^{+/+}$ mice but not in *p53*$^{-/-}$ mice. Notably, *Ass1*$^{+/-}$ mice exhibited hypersensitivity to whole-body irradiation owing to increased apoptosis in the small intestinal crypts. Analyses of *ASS1*-deficient cells generated using the CRISPR (clustered regularly interspaced short palindromic repeats)–Cas9 (CRISPR-associated 9) system revealed that ASS1 plays a pivotal role in limiting Akt phosphorylation. In addition, aberrant activation of Akt resulting from *ASS1* loss disrupted Akt-mediated cell survival signaling activity under genotoxic stress. Building on these results, we demonstrated that p53 induced an intrinsic Akt repressor, ASS1, and the perturbation of ASS1 expression rendered cells susceptible to genotoxic stress. Our findings uncover a new function of p53 in the regulation of Akt signaling and reveal how p53, ASS1, and Akt are interrelated to each other.

INTRODUCTION

p53 is involved in several cellular functions, including cell cycle arrest, senescence, and apoptosis, to prevent tumor formation (*1*). However, recent studies have shown that other p53 functions also contribute importantly to its tumor suppression activity. In particular, p53-mediated metabolic rearrangement has been revealed as a core of the p53-mediated tumor suppression system (*2*, *3*). Metabolites function as materials that build the cellular structure and also as signaling cues to modulate various cellular functions via fine-tuning of their constituent signaling components (*4*). Therefore, together with canonical p53 functions, p53-mediated metabolic rearrangement plays a pivotal role in the reconstitution of signaling network that is imperative to execute appropriate tumor suppression functions.

Cancer cells continuously modify various metabolic pathways to meet changing metabolic demands determined by cellular and environmental alterations (*5*). Thus, some nonessential amino acids become critical to survival of cancer cells. Many cancer cells cannot grow in the absence of arginine, asparagine, serine, and leucine (*6–9*). Therefore, deprivation of these amino acids has grown as an attractive therapeutic strategy for treating cancer. Among these amino acids, arginine is the most fascinating for innovative cancer therapy, and arginine starvation therapy has reached clinical trials (*9*, *10*). In arginine deprivation–based treatment, *argininosuccinate synthase 1* (*ASS1*) is one of the most critical biomarkers of sensitivity to the treatment (*11*). *ASS1* encodes the enzyme that catalyzes argininosuccinate formation from citrulline and aspartate, the rate-limiting step of de novo arginine synthesis in the urea cycle (*12*). Notably, many cancers lose the ability to synthesize arginine because of epigenetic silencing of the *ASS1* promoter (*13*), which leads

to enhanced sensitivity toward arginine deprivation. Although *ASS1* behaves as a tumor suppressor in some type of tumors (*14*, *15*), its relationship to p53, a core tumor suppressor, remains obscure.

Here, we have demonstrated that, in response to genotoxic stress, p53 directly promotes *ASS1* expression, resulting in an increase in ASS1 activity. Thus, p53-mediated *Ass1* induction is a systemic response to genotoxic stress, leading to rearrangement of arginine metabolism at the level of the whole organism in mice. We also found that ASS1 suppressed anomalous Akt phosphorylation caused by genotoxic stress that was otherwise rendering cells susceptible to genotoxic stress–triggered cell death. Our results reveal a new network topology in p53-mediated metabolic rearrangement and connect p53 and ASS1 to Akt signaling.

RESULTS

Identification of *ASS1* as a p53-activated gene

To elucidate the precise functions of p53, we conducted transcriptome and proteome analyses of human colorectal carcinoma cell line HCT116 *p53*$^{+/+}$ and HCT116 *p53*$^{-/-}$ cells at 0, 12, 24, and 48 hours after treatment with Adriamycin (ADR; also known as doxorubicin; Fig. 1A). We identified 47,534 and 19,004 peaks corresponding to 22,276 genes and 3342 proteins from transcriptome (table S1) and proteome analysis (table S2), respectively. Of the proteins from the proteome analysis, 97.6% were present in the transcriptome data. Through the transcriptome analyses, we identified 79, 295, and 203 genes as candidates for increased p53-dependent expression at 12, 24, and 48 hours after ADR treatment, respectively (fig. S1). Proteome analysis identified 36, 82, and 72 candidate p53 target proteins at 12, 24, and 48 hours after ADR treatment, respectively (fig. S1). Multiple genes in the canonical p53 signaling pathway were identified by our criteria, including *cyclin-dependent kinase inhibitor 1A* (*CDKN1A*; encoding *p21*) (*16*), *phosphate-activated mitochondrial glutaminase* (*GLS2*) (*17*), *mouse double minute 2 homolog* (*MDM2*) (*18*), and *peptidyl arginine deiminase*
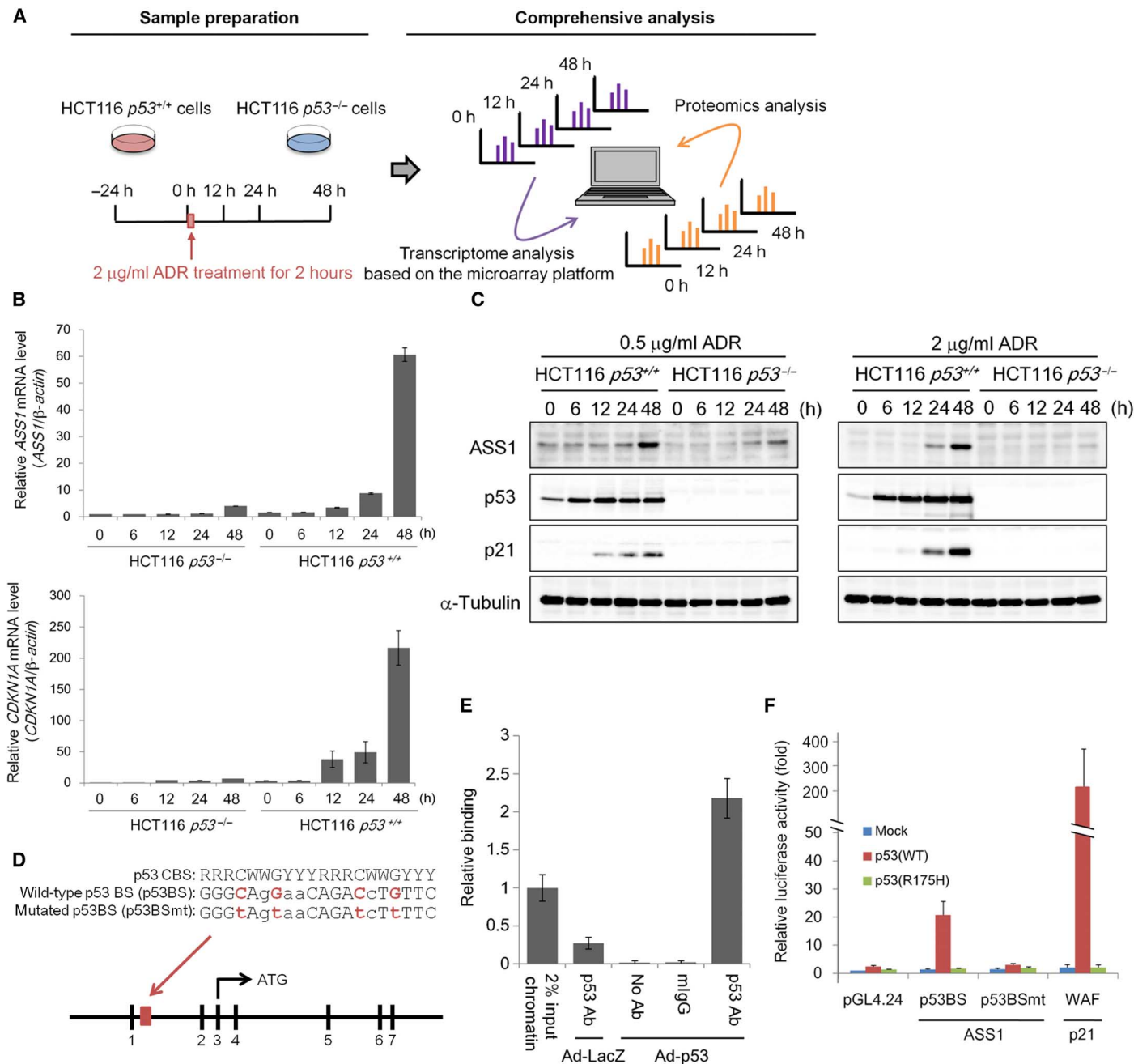
Fig. 1. Identification of *ASS1* as a direct target of p53. (**A**) Schematics of the integrated OMICS approach. HCT116 *p53*^{+/+} and HCT116 *p53*^{−/−} cells were treated with ADR (2 μg/ml) for 2 hours and then cultured with fresh medium. Cells were collected after the treatment at the indicated time and subsequently subjected to transcriptome and proteome analysis. (**B**) Expression levels of *ASS1* mRNA (top) and *p21/CDKN1A* mRNA (bottom) in cells treated with ADR (2 μg/ml) as in (A) were determined by qPCR analysis. Data were normalized by β-*actin* and presented as means ± SEM of triplicate samples relative to HCT116 *p53*^{−/−} cells without ADR treatment (0 hour). (**C**) HCT116 *p53*^{+/+} and HCT116 *p53*^{−/−} cells treated with ADR (0.5 or 2 μg/ml) as in (A) were harvested at the indicated time points and analyzed by Western blotting. (**D**) Schematic diagram of p53 binding site and sequence on the human *ASS1* gene. The identified p53 binding sequence was compared with the consensus binding sequence (CBS) (R, A/G; W, A/T; Y, C/T; nucleotides C and G in red are essential for p53 binding). Exon 3 contains the start codon. The sequences of the wild-type (p53BS) and mutated (p53BSmt) p53 binding site in intron 1 of the human *ASS1* gene were shown. (**E**) ChIP assay was performed using U373MG cells infected with adenoviruses expressing either LacZ (lane 2) or wild-type p53 (lanes 1 and 3 to 5) at a multiplicity of infection (MOI) of 10. DNA-protein complexes were immunoprecipitated with an anti-p53 antibody (Ab) (lanes 2 and 5), followed by qPCR analysis. Input chromatin represents a small portion (2%) of the sonicated chromatin before immunoprecipitation (lane 1). Immunoprecipitates with normal mouse immunoglobulin G (mIgG; lane 4) or in the absence of antibody (lane 3) were used as negative controls. Data were normalized to input chromatin (lane 1). All data are presented as means ± SD. (**F**) p53 activates luciferase activity of a reporter vector containing the p53 binding site in intron 1 of the *ASS1* gene. U373MG cells were cotransfected with the luciferase reporter vectors and vectors expressing either wild-type p53 (WT) or mutant p53 protein (R175H) 48 hours before measuring luciferase activities. Luciferase activity was normalized to the control (pGL4.24 + mock vector). The mutant p53 (R175H) was used as a negative control. Data are presented as means ± SD from three independent experiments. The sequences of p53BS and p53BSmt are shown in (D).

type IV (*PADI4*) (*19*) (tables S1 and S2), indicating the fidelity of this screening strategy. Individually, the transcriptome and proteome analyses each indicated different sets of p53 target gene candidates, whereas combined transcriptome and proteome analyses identified *ASS1*, *EPPK1*, *EPS8L2*, *APOBEC3C*, *FDXR*, *MDM2*, and *RRM2B* as common p53 target gene candidates (fig. S1 and tables S1 and S2).

One interesting gene among the seven common candidates was *ASS1*, which encodes the enzyme that catalyzes argininosuccinate formation from citrulline and aspartate, the rate-limiting step of de novo arginine synthesis in the urea cycle (*12*). Although a previous report indicates that p53 binds to a site remote from the transcription start site (TSS) of the *ASS1* gene (>116 kb from TSS) (*20*), it remains unclear whether p53 directly transactivates *ASS1*. In agreement with our transcriptomic and proteomic analyses, p53-dependent induction of *ASS1* was verified by quantitative polymerase chain reaction (qPCR) (Fig. 1B) and Western blot analysis (Fig. 1C) in ADR-treated HCT116 cells. Similarly, *ASS1* mRNA expression was increased in HCT116 cells after x-ray irradiation and treatment with Nutlin-3a, a selective small-molecule antagonist of MDM2 (*21*), in a p53-dependent manner (fig. S2). Arginine starvation did not show p53-dependent *ASS1* mRNA induction in HCT116 cells (fig. S2). Furthermore, we confirmed that *ASS1* mRNA expression was increased after the transduction of adenovirus expressing wild-type p53 in H1299 (*p53* null) and U373MG (mutated *p53*) cells (fig. S3A). In addition, ADR treatment–induced *ASS1* mRNA expression was markedly abrogated by p53 knockdown in HCT116 (wild-type p53) cells (fig. S3B). This p53-dependent induction of *ASS1* was also observed in other cell lines with wild-type p53 (fig. S3C), suggesting that p53-mediated ASS1 expression is a common mechanism underlying genotoxic stress response.

The first intron of the human *ASS1* gene (929 to 948 bases from TSS) on chromosome 9q34.1 contains a DNA fragment that closely matches the consensus p53-binding sequence (Fig. 1D) (*22*). Results of subsequent chromatin immunoprecipitation (ChIP) assays revealed that both endogenous and exogenous human p53 are recruited to this DNA fragment (Fig. 1E and fig. S4A). *ASS1* transactivation by p53 through this binding site was confirmed using luciferase assays (Fig. 1F and fig. S4B). In sum, *ASS1* was confirmed to be a direct downstream target of p53, although the extent to which *ASS1* was up-regulated differed depending on the cell type and stress input.

Regulation of arginine metabolism by the p53-ASS1 pathway

Like ASS1, several p53 targets, including GLS2 (*17*), ALDH4A1 (*23*), and PRODH/PIG6 (*24*), that regulate amino acid metabolism were enriched in the vicinity of mitochondria (fig. S5), suggesting that the modification of amino acid metabolism in and around mitochondria is a core component of the p53-mediated stress response. To investigate the role of the p53-ASS1 pathway in arginine metabolism, we measured the rates of argininosuccinate synthesis from citrulline and aspartate in HCT116 $p53^{+/+}$ and HCT116 $p53^{-/-}$ cells with or without ADR treatment. We found that ASS1 activity was significantly increased in HCT116 $p53^{+/+}$ cells, but not in HCT116 $p53^{-/-}$ cells, in response to genotoxic stress (Fig. 2A and fig. S6A). To exclude the possibility that other p53-inducible gene products are involved in the metabolic process, ASS1 activity was examined in HCT116 cells, in which *ASS1* was knocked out using the CRISPR (clustered regularly interspaced short palindromic repeats)–Cas9 (CRISPR-associated 9) genome editing system (sgASS1 cells) (fig. S6B). HCT116 cells, whose *AAVS1* safe harbor locus is edited by the CRISPR-Cas9 system, were used as control cells (AAVS1 cells). As shown in Fig. 2B, increase in ASS1 activity by ADR-induced genotoxic stress was diminished in *ASS1*-deficient sgASS1 cells. These results show that p53 promotes de novo arginine synthesis pathway via *ASS1* induction in response to genotoxic stress.

Systemic regulation of *Ass1* by p53 in x-ray–irradiated mice

Although it is known that *Ass1* is ubiquitously expressed in various tissues, with its most abundant expression in the liver and kidney (*25*), the regulatory mechanism of *Ass1* in response to genotoxic stress
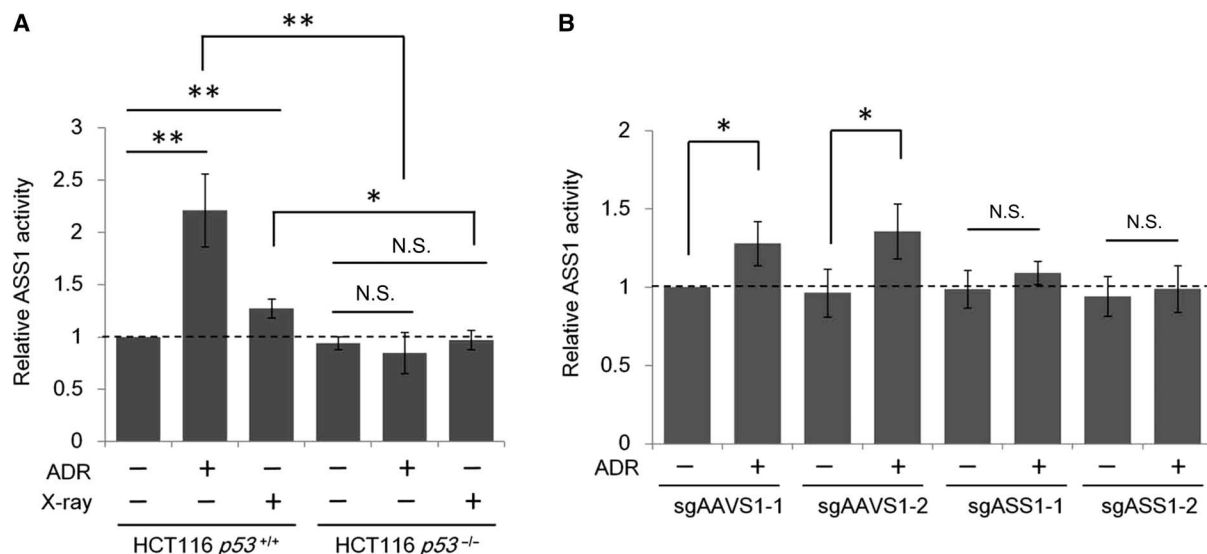

Fig. 2. p53 regulates arginine metabolism through ASS1. (**A**) For ADR treatment, HCT116 $p53^{+/+}$ and HCT116 $p53^{-/-}$ cells were treated with ADR (2 μg/ml) for 2 hours and then cultured with fresh medium. For x-ray irradiation, the cells were irradiated with 20 gray (Gy) of x-ray. At 48 hours after treatment, cells were subjected to an in vitro ASS1 activity assay. Data are normalized to control HCT116 $p53^{+/+}$ cells (lane 1) and presented as means ± SD from three independent experiments. (**B**) sgAAVS1 (HCT116 $ASS1^{+/+}$) and sgASS1 (HCT116 $ASS1^{-/-}$) cells were treated with ADR (2 μg/ml) as in (A). At 48 hours after treatment, cells were subjected to an in vitro ASS1 activity assay. Data are normalized to control sgAAVS1-1 cells (lane 1) and presented as means ± SD from three independent experiments. *$P < 0.05$; **$P < 0.01$; N.S., not statistically significant.

at the level of the whole organism remains unclear. To clarify the systemic regulation of *Ass1* under genotoxic conditions, *Ass1* mRNA levels were investigated by RNA sequencing (RNA-seq) in various tissues of $p53^{+/+}$ and $p53^{-/-}$ mice after exposure to total body x-ray irradiation (TBI). *Cdkn1a*, a major p53 target, showed significantly higher expression levels in $p53^{+/+}$ mice than in $p53^{-/-}$ mice after TBI in all analyzed tissues (fig. S7), indicating the feasibility of this approach. Consistent with the previous report, basal *Ass1* mRNA was more abundant in kidney and liver than in other tissues in both $p53^{+/+}$ and $p53^{-/-}$ mice (Fig. 3A). Notably, various tissues, including heart, spleen, and small intestine, showed a significant increase in *Ass1* mRNA expression after TBI in $p53^{+/+}$ mice compared to that of $p53^{-/-}$ mice (Fig. 3A). Induction of Ass1 protein was also confirmed in the thymus and small intestine of $p53^{+/+}$ mice (fig. S8). On the other hand, *Ass1* mRNA in kidney and liver did not increase after TBI, irrespective of *p53* status (Fig. 3A). These results indicate that p53 transactivates *Ass1* in various

tissues in response to genotoxic stress, although the extent of its induction differs depending on tissues.

The tissue-specific expression patterns of *Ass1* by p53 led us to speculate that versatile gene network patterns underlying the regulation of arginine metabolism were created in different tissues under genotoxic condition. To address this possibility, we examined the expression level of arginine metabolism–related genes under genotoxic condition. RNA-seq data revealed that arginine metabolism–related genes showed obvious differences after TBI in various tissues of $p53^{+/+}$ mice but not in $p53^{-/-}$ mice (Fig. 3B). Notably, *Ass1* and *Arginase 2* (*Arg2*), key enzymes in arginine metabolism, showed similar expression pattern in various tissues of $p53^{+/+}$ mice, suggesting that genotoxic stress switched on the arginine anabolic process (mediated by Ass1) and catabolic process (mediated by Arg2) concomitantly as a systemic response to genotoxic stress. Because genotoxic stress–induced *Arg2* induction was observed in HCT116 cells irrespective of
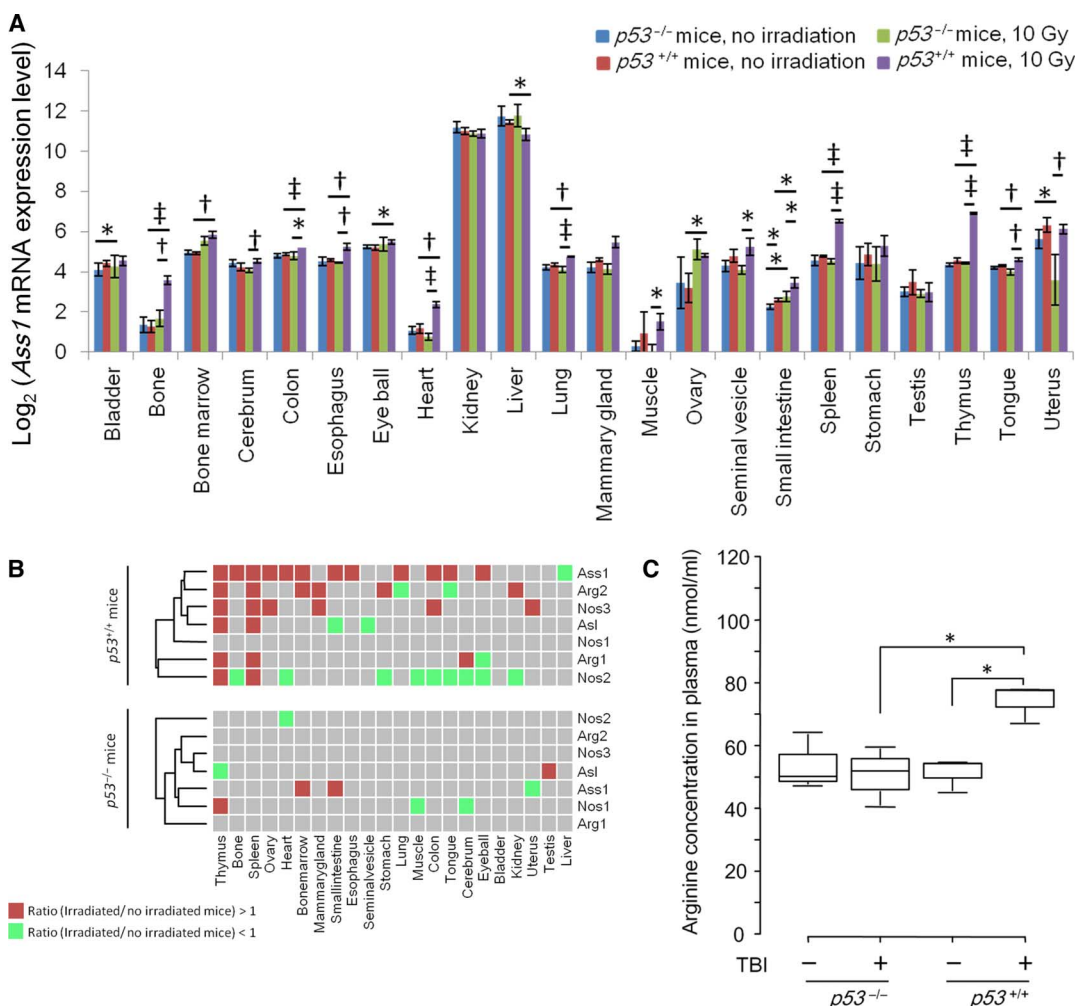

Fig. 3. p53 systemically regulates *Ass1* expression in response to genotoxic stress in mice. (**A**) At 24 hours after 10 Gy of TBI, expression levels of *Ass1* mRNA in various tissues of $p53^{+/+}$ and $p53^{-/-}$ mice were measured by RNA-seq. Graph shows means ± SD [each group, $n = 3$ (mammary gland and ovary, $n = 2$)]. *$P < 0.05$; †$P < 0.01$; ‡$P < 0.001$. (**B**) At 24 hours after 10 Gy of TBI, expression levels of arginine metabolism–related genes in various tissues of $p53^{+/+}$ and $p53^{-/-}$ mice were measured by RNA-seq. Gray: No significant difference between control mice and irradiated mice. (**C**) Box plots show the concentration of plasma arginine in $p53^{+/+}$ mice and $p53^{-/-}$ mice 24 hours after 10-Gy TBI. $p53^{+/+}$ mice, no irradiation, $n = 3$; $p53^{-/-}$ mice, no irradiation, $n = 3$; $p53^{+/+}$ mice, TBI, $n = 3$; $p53^{-/-}$ mice, TBI, $n = 4$. *$P < 0.05$, one-way analysis of variance (ANOVA) with Bonferroni multiple comparison test.

the p53 status (table S1), the simultaneous regulation of Ass1 and Arg2 might be species- and/or tissue-specific.

Several lines of evidence indicate that changes in plasma amino acid levels reflect systemic changes in metabolism (26–28). Because p53 promoted ASS1 activity in vitro (Fig. 2), we hypothesized that systemic Ass1 induction with fine-tuned regulation of arginine metabolism–related genes changes the plasma arginine level. To examine the hypothesis, we measured plasma arginine level after TBI and found that only irradiated $p53^{+/+}$ mice show a significant increase of plasma arginine level in response to genotoxic stress (Fig. 3C). This effect in $p53^{+/+}$ mice might be, at least partially, explained by the systemic induction of Ass1 and rearrangement of arginine metabolism after TBI. Together, these results suggested that p53 regulates a set of arginine metabolism–related genes including Ass1 and plays a pivotal role in arginine metabolism at the level of the whole organism in mice.

Ass1 is a key molecule to alter irradiation sensitivity in mice

Although p53 is a determinant of radiation syndrome (29), the details of the mechanism remain to be elucidated. Emerging evidence has revealed that arginine has antioxidant properties (30, 31); thus, arginine supplementation exhibited a protective effect against radiation toxicity (32–34). Accordingly, we assumed that Ass1 might be a key molecule to determine the sensitivity toward genotoxic stress. To dissect how Ass1 functions at the whole-body level as a downstream p53 target, we investigated the effect of Ass1 loss on the genotoxic stress response. Because $Ass1^{-/-}$ mice died within few days after birth (35), $Ass1^{+/-}$ mice and genetically matched wild-type counterparts were subjected to the experiments. As expected, the expression level of Ass1 mRNA and Ass1 protein was notably lower in $Ass1^{+/-}$ mice than in wild-type counterparts (fig. S9A). To further characterize loss of Ass1 in heterogenic mice, we examined the citrulline level in plasma, motivated by the fact that ASS1 is a gene responsible for citrullinemia type I, an autosomal recessive genetic disorder (36). As expected, the citrulline concentration in plasma was significantly greater in $Ass1^{+/-}$ mice compared with wild-type counterparts (fig. S9B), indicating that heterogenic loss of Ass1 was enough to perturb Ass1-mediated arginine metabolism in mice. Notably, the metabolic change observed in $Ass1^{+/-}$ mice did not exhibit any obvious adverse effects, as determined by clinical chemistry parameters (fig. S9C).

We subsequently examined the effect of TBI on survival and found that $Ass1^{+/-}$ mice showed higher sensitivity to 10 Gy of x-ray irradiation compared with wild-type counterparts (Fig. 4A). Notably, the plasma arginine level was almost the same between $Ass1^{+/-}$ mice and $Ass1^{+/+}$ mice irrespective of genotoxic stress (fig. S10). Nevertheless, $Ass1^{+/-}$ mice exhibited higher sensitivity toward genotoxic stress in comparison with that exhibited by $Ass1^{+/+}$ mice, suggesting that endogenous (for example, de novo arginine synthesis) and exogenous (for example, diet) arginine supplementation is required to protect mice from genotoxic stress. As expected, the arginine-free diet significantly reduced the survival of wild-type mice exposed to TBI (Fig. 4B), whereas no synergistic effect was observed in $Ass1^{+/-}$ mice fed with an arginine-free diet (fig. S11A). These results suggested that sensitivity toward genotoxic stress could be explained as Boolean NAND gate (37), where Ass1 status and diet arginine supplementation are assumed to be independent binary inputs (fig. S11B).

We next looked into the effect of TBI on tissue morphology. Consequently, we found that villi length was markedly shortened in the small intestine $Ass1^{+/-}$ mice after TBI (Fig. 4C). Likewise, hypersensitivity to radiation was also observed in the small intestine of $p53^{-/-}$

mice (29). No noticeable differences in the morphology of other tissues were noted between $Ass1^{+/+}$ and $Ass1^{+/-}$ mice after TBI (fig. S12A). Subsequent immunohistochemical analyses indicated that the numbers of terminal deoxynucleotidyl transferase–mediated deoxyuridine triphosphate nick end labeling (TUNEL)–positive cells in the small intestinal crypts of $Ass1^{+/-}$ mice were greater than those in wild-type counterparts (Fig. 4D). No obvious difference was observed between Ki67 expression in $Ass1^{+/+}$ and $Ass1^{+/-}$ mice, irrespective of TBI (fig. S12B). qPCR revealed that Ass1 mRNA expression in the small intestine of $Ass1^{+/-}$ mice was significantly lower than that in wild-type mice after TBI (fig. S13), suggesting that, at least in the small intestine, reduced expression of Ass1 promoted apoptosis in response to genotoxic stress.

ASS1 deficiency promotes Akt phosphorylation and susceptibility to ADR-induced cell death

To clarify the mechanism by which ASS1 changes sensitivity to genotoxic stress, we first examined whether ASS1-deficient sgASS1 cells also showed higher sensitivity to genotoxic stress compared with its wild-type counterparts. Consistent with $Ass1^{+/-}$ mice, ASS1 deficiency rendered cells susceptible to ADR-triggered cell death (Fig. 5A). A similar phenotype was also observed in Ass1-deficient mouse embryonic fibroblasts (MEFs; Fig. 5B), indicating that ASS1 plays an important role in defining sensitivity to genotoxic stress.

We next examined Akt and the downstream mechanistic target of rapamycin (mTOR) complex 1 (mTORC1) pathway, whose phosphorylation statuses are variable in response to genotoxic stress (38). Consistent with a previous report (39), genotoxic stress promoted the phosphorylation of Akt in wild-type cells (Fig. 5C). Notably, ASS1-deficient cells exhibited increased basal Akt phosphorylation, and the phosphorylation level increased enormously under genotoxic conditions, in which the p53-ASS1 pathway was completely blocked (Fig. 5C). ASS1 overexpression suppressed genotoxic stress–induced Akt phosphorylation in both sgAAVS1 and sgASS1 cells (fig. S14A), suggesting that ASS1 plays a role in inhibiting Akt. The contribution of Ass1 loss to elevated Akt phosphorylation was also observed in Ass1-deficient MEFs (fig. S15). These observable changes in Akt phosphorylation occurred in an mTORC1-independent manner (Fig. 5C and fig. S15). These results indicate that p53 downstream gene product ASS1 is a crucial repressor for Akt phosphorylation. Notably, p53-deficient cells did not show an increase in Akt phosphorylation in response to genotoxic stress (fig. S16), probably through a negative feedback mechanism, because increased mTORC1 activity that was determined by phosphorylation of downstream substrate p70 S6K1 (ribosomal S6 protein kinase 1) was shown to limit Akt phosphorylation (40).

In addition to the mTORC1/p70 S6K1–mediated negative feedback loop, the major Akt S473 kinase mTORC2 is also involved in increasing Akt phosphorylation (41). To examine which pathways were involved in ADR-induced Akt phosphorylation, cells were treated with the rapamycin (mTORC1 inhibitor) and mTOR inhibitors PP242 and Torin2. In these experiments, PP242 and Torin2, but not rapamycin, inhibited ADR-induced Akt phosphorylation (Fig. 5D). These results indicate that mTORC2, rather than the mTORC1/p70 S6K1–dependent negative feedback loop, is responsible for Akt phosphorylation induced by genotoxic stress.

It has been reported that Akt phosphorylation status defines functional outputs of Akt: Once Akt phosphorylation level exceeds the defined threshold, it triggers cell death (42). To examine whether aberrant Akt activation found in ASS1-deficient cells promoted ADR-induced cell death, cells were cultured with a low concentration

of Akt inhibitor that was sufficient to reduce ADR-induced Akt phosphorylation (Fig. 5E) without affecting basal cell growth (Fig. 5F). Under this condition, the Akt inhibitor partially rescued ADR-induced cell death in *ASS1*-deficient cells but not in wild-type cells (Fig. 5F). Consistent with these results, ASS1 overexpression, which also suppressed genotoxic stress–induced Akt phosphorylation (fig. S14A), protected cells against genotoxic stress, especially sgASS1 cells (1.36 ± 0.04–fold recovery in sgAAVS1 cells and 1.68 ± 0.1–fold recovery in sgASS1 cells; *P* < 0.01, Student's *t* test) (fig. S14B). These results suggest that the hyperphosphorylation of Akt observed in *ASS1*-deficient cells contributed at least partially to the increase in sensitivity to genotoxic stress.

Arginine insufficiency promotes Akt phosphorylation

The fact that *ASS1*-deficient cells were arginine-auxotrophic (*43*) led us to consider the possibility that *ASS1*-deficient cells would be unable to synthesize enough arginine to keep up with the de-mand, thus resulting in elevated Akt phosphorylation. To address this question, we looked into the effect of arginine insufficiency on Akt phosphorylation. We found that Akt phosphorylation at T308 and S473 increased under arginine starvation (Fig. 6A), whereas subsequent arginine supplementation suppressed arginine withdrawal–induced Akt phosphorylation at S473, but not at T308, within 4 hours (Fig. 6B). Similar to ADR treatment, Akt phosphorylation in *ASS1*-deficient cells was highly sensitive to arginine withdrawal than in wild-type cells (Fig. 6, A and B).

Because ADR treatment caused intracellular amino acid insufficiency (*44*), we assumed that arginine insufficiency triggered Akt phosphorylation in ADR-treated cells. As expected, arginine supplementation suppressed genotoxic stress–induced Akt phosphorylation (fig. S17A). In addition, arginine supplementation prevented genotoxic stress–induced death, especially, of sgASS1 cells (1.19 ± 0.08–fold recovery in sgAAVS1 cells and 1.39 ± 0.06–fold recovery in sgASS1 cells; *P* < 0.05, Student's *t* test) (fig. S17B).
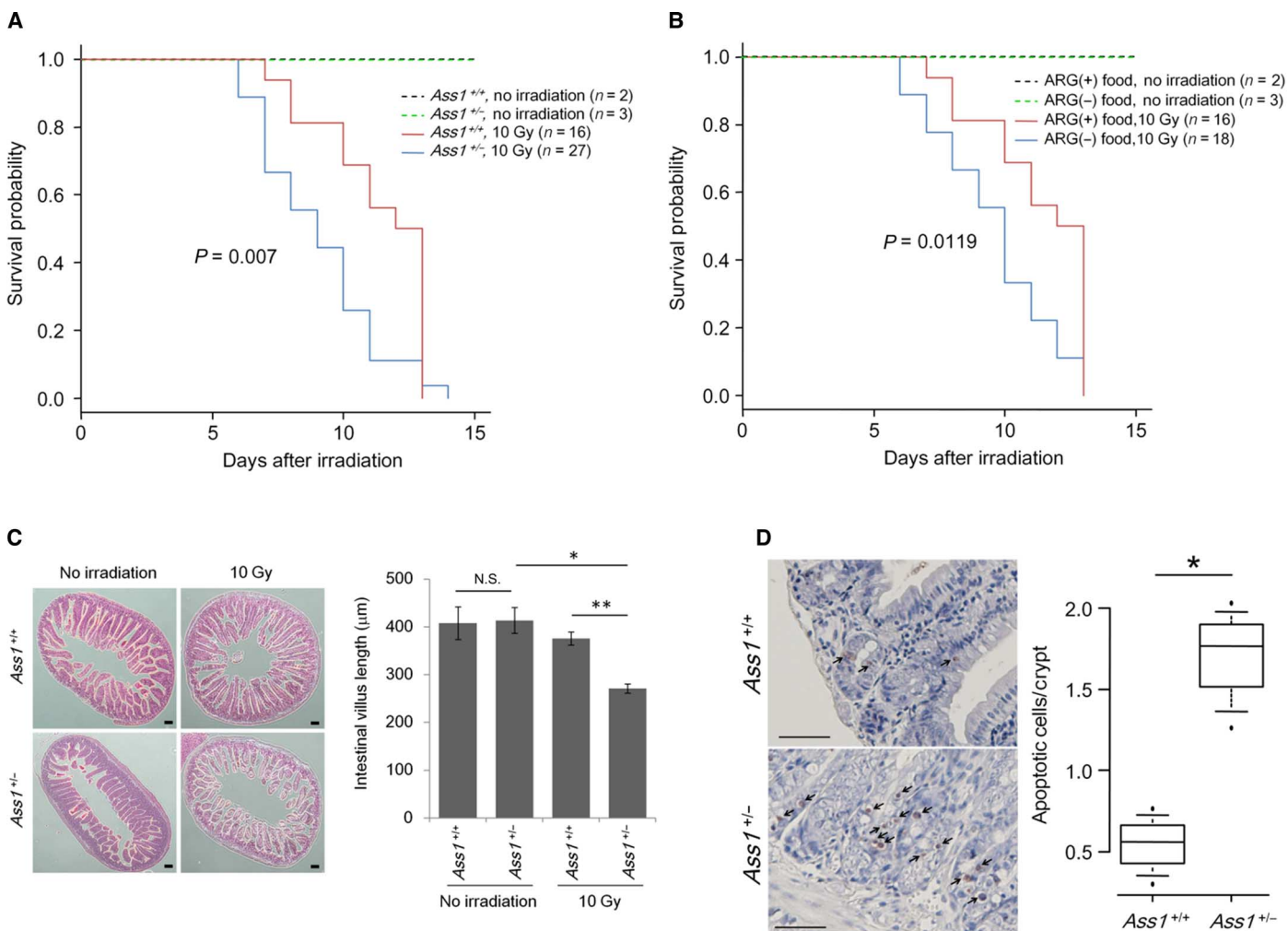

Fig. 4. Ass1 is a key molecule to alter irradiation sensitivity in mice. (**A**) Kaplan-Meier survival curves of *Ass1*^{+/+} and *Ass1*^{+/−} exposed to 10-Gy TBI. *P* values were calculated by the log-rank test. (**B**) Kaplan-Meier survival curves of *Ass1*^{+/+} mice fed with arginine-free [Arg(−)] or normal [Arg(+)] food after 10 Gy of TBI. *P* values were calculated by the log-rank test. (**C**) Left: Representative hematoxylin and eosin (H&E) staining of the small intestine in wild-type and *Ass1*^{+/−} mice 10 days after TBI. Scale bars, 100 μm. Right: The lengths of villi in *Ass1*^{+/+} (*n* = 3) and *Ass1*^{+/−} (*n* = 3) mice 10 days after 10-Gy TBI are shown as means ± SEM. *P* < 0.05; **P* < 0.01. (**D**) Left: TUNEL staining of the small intestine of *Ass1*^{+/+} and *Ass1*^{+/−} mice 24 hours after 10-Gy TBI. Arrow: TUNEL-positive cells. Scale bars, 50 μm. Right: Numbers of TUNEL-positive cells are shown as a box plot (*n* = 3 each). *P* < 0.05.
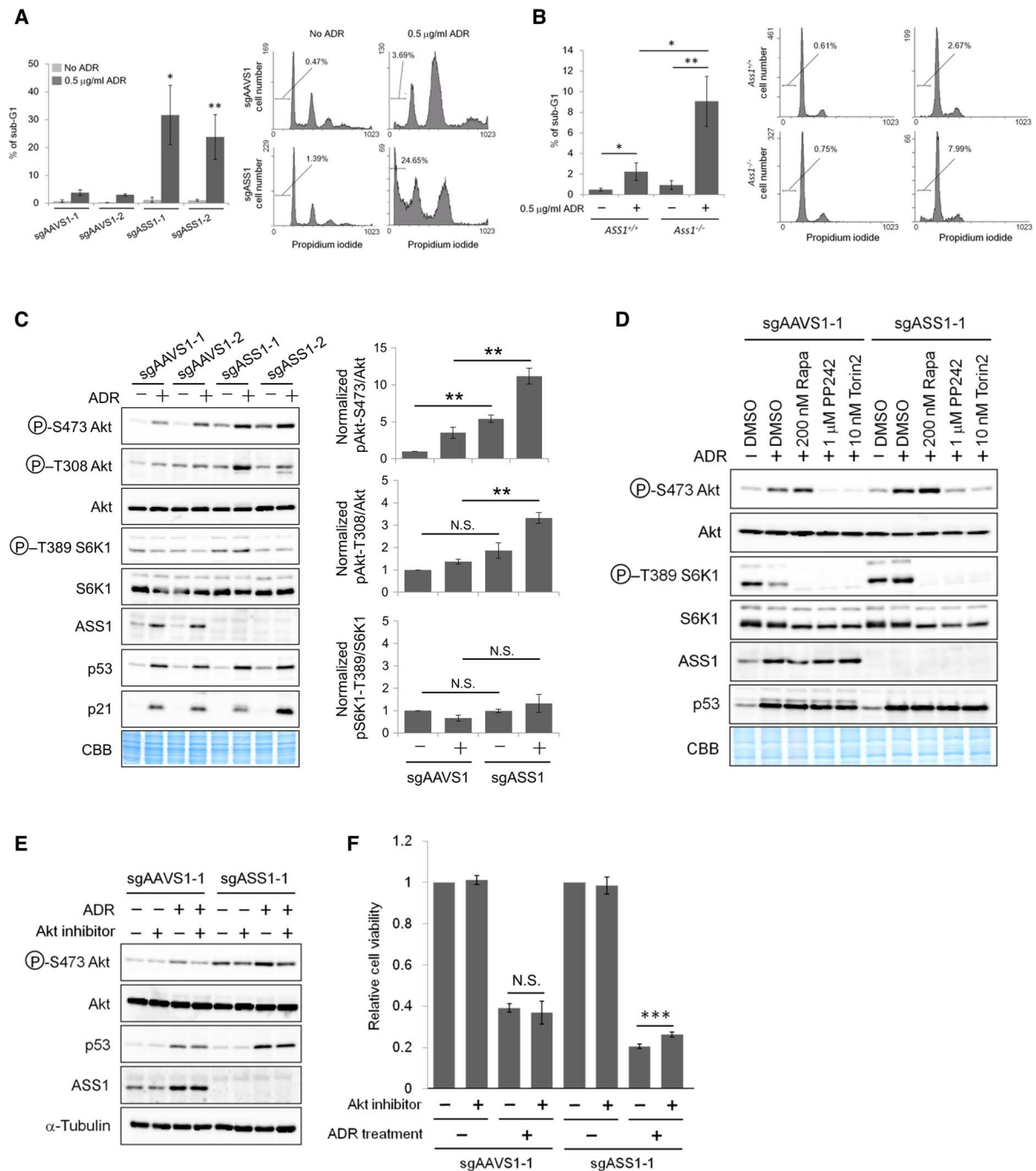
Fig. 5. *ASS1* deficiency promotes Akt phosphorylation and susceptibility to ADR-induced cell death. (**A**) sgAAVS1 (HCT116 *ASS1*^{+/+}) and sgASS1 (HCT116 *ASS1*^{−/−}) cells were treated with ADR (0.5 μg/ml) for 2 hours and then cultured with fresh medium. At 48 hours after treatment, cells were subjected to flow cytometry and analyzed. Left: Percentage of sub-G₁ cells with means ± SD ($n = 3$). *$P < 0.05$; **$P < 0.01$, compared to ADR-treated sgAAVS1-1 cells. Right: Representative histograms of flow cytometric analysis. (**B**) Wild-type *ASS1* MEFs (*Ass1*^{+/+}) and *ASS1*-deficient MEFs (*Ass1*^{−/−}) were treated with ADR (0.5 μg/ml) for 48 hours. Left: Percentage of sub-G₁ cells with means ± SD ($n = 3$). *$P < 0.05$; **$P < 0.01$. Right: Representative histograms of flow cytometric analysis. (**C**) sgAAVS1 (HCT116 *ASS1*^{+/+}) and sgASS1 (HCT116 *ASS1*^{−/−}) cells were treated with ADR (0.5 μg/ml) for 2 hours and then cultured with fresh medium. At 48 hours after treatment, the cells were subjected to Western blot analysis. The phosphorylation levels of Akt and S6K1 are shown as means ± SEM of triplicate samples relative to control sgAAVS1-1 cells (lane 1). Representative Western blot results are shown. *$P < 0.05$; **$P < 0.01$. CBB, Coomassie brilliant blue. (**D**) sgAAVS1 (HCT116 *ASS1*^{+/+}) and sgASS1 (HCT116 *ASS1*^{−/−}) cells were treated with ADR as in (C). At 42 hours after ADR treatment, cells were treated with indicated inhibitors for 6 hours. Cell lysates were analyzed by immunoblotting. DMSO, dimethyl sulfoxide; Rapa, rapamycin. (**E**) sgAAVS1-1 (HCT116 *ASS1*^{+/+}) and sgASS1-1 (HCT116 *ASS1*^{−/−}) cells were treated with ADR (0.5 μg/ml) for 2 hours and then given fresh medium containing 3 μM Akt inhibitor X. At 72 hours after treatment, the phosphorylation level of Akt S473 was analyzed by immunoblotting. (**F**) sgAAVS1-1 (HCT116 *ASS1*^{+/+}) and sgASS1-1 (HCT116 *ASS1*^{−/−}) cells were treated with Akt inhibitor X as in (E). At 72 hours after ADR treatment, cell viability assay was performed. Graphs show means ± SD from three independent experiments. ***$P < 0.001$.
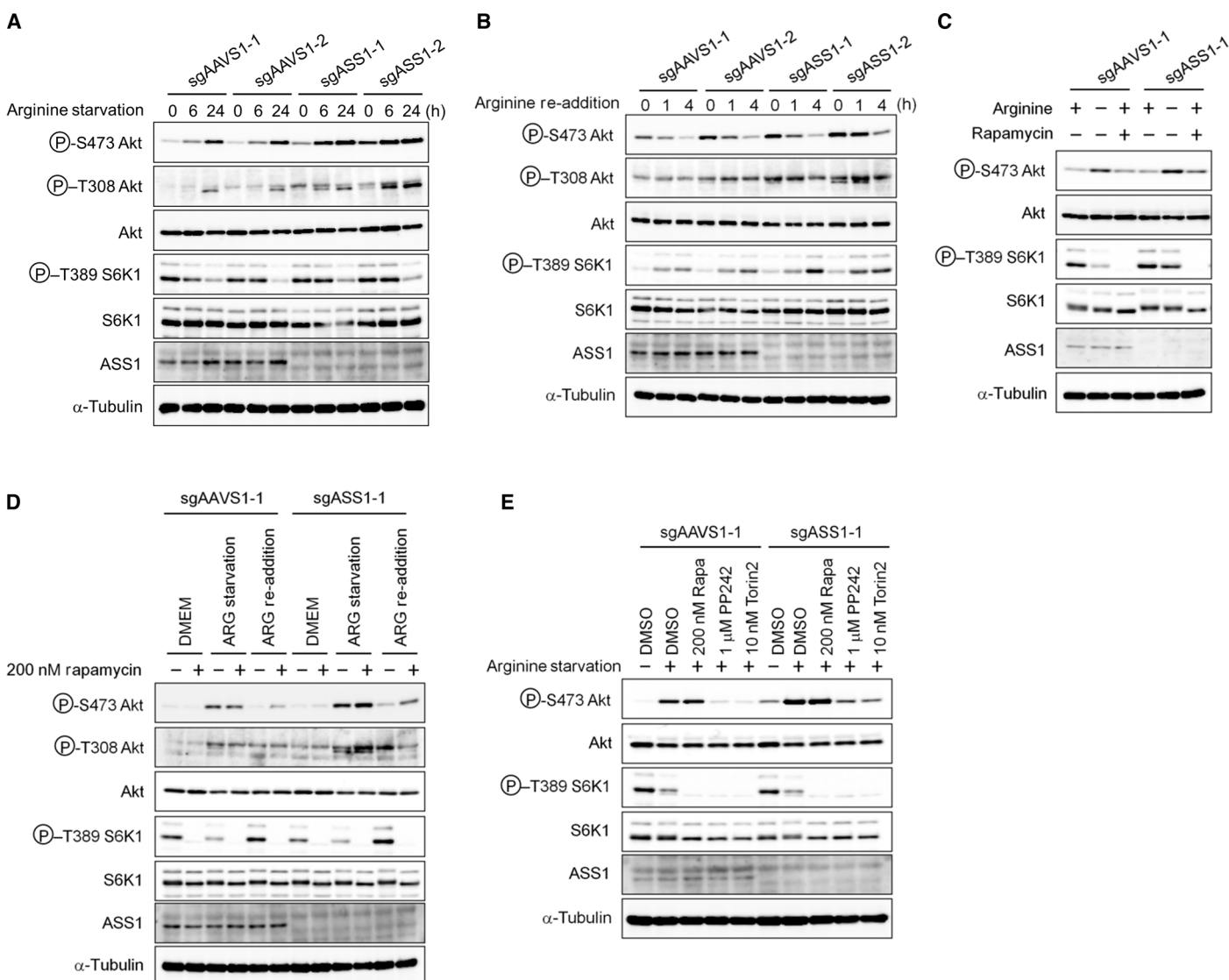
Fig. 6. Akt is an intrinsic arginine probe. (A) sgAAVS1 (HCT116 $ASS1^{+/+}$) and sgASS1 (HCT116 $ASS1^{-/-}$) cells were cultured with arginine-free medium for the indicated time. Cell lysates were analyzed by immunoblotting. **(B)** sgAAVS1 (HCT116 $ASS1^{+/+}$) and sgASS1 (HCT116 $ASS1^{-/-}$) cells were cultured with arginine-free medium for 24 hours and subsequently stimulated with arginine (final concentration, 0.398 mM) for the indicated time. Cell lysates were analyzed by immunoblotting. **(C)** sgAAVS1 (HCT116 $ASS1^{+/+}$) and sgASS1 (HCT116 $ASS1^{-/-}$) cells were cultured under the indicated condition for 4 hours. Cell lysates were analyzed by immunoblotting. Rapamycin, 200 nM. **(D)** sgAAVS1 (HCT116 $ASS1^{+/+}$) and sgASS1 (HCT116 $ASS1^{-/-}$) cells were cultured with arginine-containing or arginine-free medium for 20 hours and then treated with the indicated conditions for 4 hours. Cell lysates were analyzed by immunoblotting. DMEM, Dulbecco's modified Eagle's medium. **(E)** sgAAVS1 (HCT116 $ASS1^{+/+}$) and sgASS1 (HCT116 $ASS1^{-/-}$) cells were cultured with arginine-free medium for 18 hours and subsequently treated with the indicated mTOR inhibitor for 6 hours. Cell lysates were analyzed by immunoblotting.

Arginine is the primary amino acid monitored by mTORC1 (45), whose inactivation disconnects the mTORC1-Akt negative feedback loop and leads to increased Akt phosphorylation (46). To assess the effects of the mTORC1-Akt negative feedback loop on arginine-mediated Akt phosphorylation, cells were treated with the mTORC1 inhibitor rapamycin. Although mTORC1 activity was completely suppressed by rapamycin and not by arginine starvation, we found that arginine deprivation triggered Akt phosphorylation to a larger extent than that induced by rapamycin (Fig. 6C). In addition, subsequent arginine supplementation suppressed phosphorylation at Akt S473, but not at T308, despite the presence of rapamycin (Fig. 6D). These data suggest that the arginine level directly translated to the physiological

input information that regulates Akt phosphorylation. Furthermore, we demonstrated that arginine starvation–induced phosphorylation of Akt at S473 was markedly suppressed by PP242 and Torin2, but not rapamycin (Fig. 6E). Together, these results suggested that mTORC2 senses arginine insufficiency and then promotes Akt S473 phosphorylation.

DISCUSSION
Although accumulating evidence highlights the importance of p53-mediated metabolism in tumor suppression (2, 47), the mechanisms by which p53 drives dynamic nutrient status in harmony with canonical

p53 functions remain poorly understood. Here, we show that p53 activates the penultimate step of de novo arginine synthesis pathway through the direct induction of the rate-limiting enzyme *ASS1*. Furthermore, we demonstrate that *ASS1* deficiency induced anomalous Akt phosphorylation, resulting in rendering cells more susceptible to genotoxic stress.

Although we have demonstrated that p53 drives the de novo arginine synthesis pathway via *ASS1* induction under genotoxic conditions, *argininosuccinate lyase* (*ASL*), which directly produces arginine from argininosuccinate, was not induced by p53 in HCT116 cells. These results suggest that ASS1 is the sole node connecting p53 to the de novo arginine synthesis pathway. Because ASS1 is a rate-limiting enzyme of the de novo arginine synthesis pathway, ASS1 induction might be enough to meet arginine demand under genotoxic conditions. We note that although genotoxic stress–induced ASS1 expression by p53 resulted in increased ASS1 activity, we could not detect decreased ASS1 activity in *ASS1*-deficient sgASS1 cells compared with wild-type AAVS1 cells under steady-state conditions. One speculation is that the ASS1 expression level in sgAAVS1 cells might be lower than the limit of detection of the in vitro ASS1 activity assay, resulting in the lack of an obvious difference in ASS1 activity between sgAAVS1 and sgASS1 cells. Another possibility is that p53-dependent posttranslational modifications of ASS1 might change ASS1 activity in accordance with the increase in its expression level under genotoxic conditions. Various posttranslational modifications of ASS1 have been reported in PhosphoSitePlus (www.phosphosite.org/homeAction.action), a comprehensive resource devoted to information regarding posttranslational modifications (*48*). Further studies are therefore necessary to resolve the molecular mechanism underlying ASS1 activity regulation.

Although p53 was a major transcription factor responsible for inducing *ASS1* mRNA under genotoxic conditions, a slight induction of ASS1 was observed in HCT116 *p53*$^{-/-}$ cells after prolonged ADR treatment. Thus, we assume that other transcription factor(s) may function in ASS1 regulation with p53 under genotoxic stress to a slight extent. Until now, three transcription factors (c-Myc, HIF-1α, and Sp4) have been reported to be involved in the regulation of ASS1 (*49*). Untangling the relationship between p53 and other transcription factors will help elucidate the regulatory mechanism of ASS1 under various conditions.

In the last decade, arginine has garnered interest as a metabolite encoding multiple pieces of information (*50–52*). Arginine and its metabolites, including nitric oxide (NO), polyamines, glutamine, and creatine, have very important biological functions (*51*). Thus, the p53-ASS1 pathway could regulate various cellular functions by propagating these metabolites as input information.

Akt is a key hub molecule that is activated in many tumors (*53*). In agreement with previous studies showing that p53 suppresses Akt activity via PTEN (*54*) and PHLDA3 (*55*), we found that a new p53-activated gene product, ASS1, was also an intrinsic Akt repressor. Notably, the mechanisms by which these Akt repressors disabled Akt were different: PTEN and PHLDA3 blocked Akt phosphorylation by repressing the phosphatidylinositol 3,4,5-trisphosphate signal input, whereas ASS1 prevented arginine insufficiency–induced Akt phosphorylation that was more sensitive to the arginine level than p70 S6K1, a major amino acid probe regulated by mTORC1 (*46*). However, the mechanism by which Akt senses intracellular and extracellular arginine level remains elusive. Notably, arginine supplementation succeeded in suppressing Akt phosphorylation and in preventing genotoxic stress–induced cell death; the effect

was observed in both *ASS1*-deficient cells and their wild-type counterparts. In addition, arginine supplementation did not completely suppress elevated Akt phosphorylation in *ASS1*-deficient cells. These results imply that arginine derived from the de novo arginine synthesis system and other sources might have different physiological roles to some extent. A similar complex mechanism of arginine utilization is also observed in the regulatory system of NO synthase (known as the arginine paradox) (*56*). Therefore, further experiments are necessary to resolve the molecular mechanisms underlying the relationships between arginine metabolism and Akt signaling.

Our results also demonstrate that *ASS1* deficiency sensitizes cells to genotoxic stress–induced cell death both in vitro and in vivo. Moreover, suppression of Akt phosphorylation significantly suppresses ADR-induced death of *ASS1*-deficient cells. Therefore, increased sensitivity to genotoxic stress in *ASS1*-deficient cells is explained by abnormal Akt phosphorylation. Notably, although the small intestine of *Ass1*$^{+/-}$ mice exhibited higher sensitivity to TBI, as judged by the number of apoptotic cells, we could not detect an obvious difference in Akt phosphorylation in the small intestine of *Ass1*$^{+/+}$ and *Ass1*$^{+/-}$ mice after TBI, because the most likely cause is the limitation of antibody affinity (data not shown).

Cell death driven by the abnormal Akt phosphorylation was observed and supported by the previously advocated "switching model," which postulates that Akt reconstructs its signaling network from cell survival output to cell death output concomitantly with its anomalous phosphorylation status (*42*). As a potential explanation for the switching mechanism of Akt outputs, the spatiotemporal activation dynamics of Akt signaling might be perturbed when p53-mediated Akt repression system was inactivated. Because Akt signaling is spatiotemporally compartmentalized within a cell (*57*, *58*), a deep understanding of Akt activation dynamics at the subcellular compartment level might reveal the mechanism by which Akt assures the execution of opposite downstream functions in accordance with its phosphorylation status.

In summary, the present data demonstrate the important role of the p53-ASS1 pathway in arginine metabolism and genotoxic stress responses. Furthermore, we have found that ASS1 plays a key role in the regulation of Akt phosphorylation induced by genotoxic stress as well as arginine insufficiency. Several clinical trials have shown that arginine depletion is an effective treatment for patients with *ASS1*-negative tumors (*59*). We believe that our study provides evidence for the potential of p53- and ASS1-targeted cancer therapies and possible explanations for resistance to such treatments.

MATERIALS AND METHODS
Cell culture and treatment
Human cancer cell lines U373MG (astrocytoma), H1299 (non–small cell lung cancer), A-427 (lung adenocarcinoma), and HCT116 (colorectal adenocarcinoma) were purchased from the American Type Culture Collection. HCT116 *p53*$^{+/+}$ and HCT116 *p53*$^{-/-}$ cell lines were gifts from B. Vogelstein (Johns Hopkins University). HEC-108 (endometrioid adenocarcinoma) was obtained from the Japanese Collection of Research Biosources Cell Bank. Human embryonic kidney (HEK) 293T and HCT116 cells were cultured in DMEM (Gibco) supplemented with 10% fetal bovine serum (FBS) and 1% penicillin/streptomycin at 37°C in 5% CO$_2$. U373MG, A427, and HEC-108 cells were cultured in minimum essential medium (Gibco) supplemented with 10% FBS and 1% penicillin/streptomycin at 37°C in 5% CO$_2$.

H1299 cells were cultured in RPMI 1640 (Gibco) supplemented with 10% FBS and 1% penicillin/streptomycin at 37°C in 5% CO_2. MEFs were cultured in DMEM supplemented with 10% FBS at 37°C in 5% CO_2. For arginine starvation, cells were cultured with arginine-free DMEM containing 10% FBS and 1% penicillin/streptomycin. HEK293T and U373MG cells were transfected with plasmids using FuGENE6 (Promega) and Lipofectamine LTX (Invitrogen), respectively. Small interfering RNA (siRNA) oligonucleotides, commercially synthesized by Sigma Genosys, were transfected with Lipofectamine RNAiMAX reagent (Invitrogen). Sequences of siRNA oligonucleotides are as follows: Si-EGFP, 5′-GCAGCACGACUUCUUCAAGT-3′ (forward) and 5′-CUUGAAGAAGUCGUGCUGC-3′ (reverse); Si-p53, 5′-GACUCCAGUGGUAAUCUACUT-3′ (forward) and 5′-AGUA-GAUUACCACUGGAGUCTT-3′ (reverse). We generated and purified replication-deficient recombinant viruses expressing p53 (Ad-p53) or LacZ (Ad-LacZ), as described previously (60). H1299 and U373MG were infected with viral solutions at various MOIs and incubated at 37°C until the time of harvest. For treatment with genotoxic stress, cells were incubated with ADR (0.5 or 2 µg/ml) for 2 hours and then given fresh medium. For x-ray irradiation, cells were irradiated by x-ray by using the MBR-1520R-3 System (Hitachi).

Materials

Anti-ASS1 (sc-46066) and anti-Akt (sc-5298) antibodies and normal mouse IgG (sc-2025) were purchased from Santa Cruz Biotechnology. Anti-p53 (OP43), anti-p53 (OP140), and anti-p21 (OP64) antibodies were purchased from Merck Millipore. Anti–β-tubulin (#2125), anti–phospho-Akt (S473) (#4060), anti–phospho-Akt (T308) (#5106), anti–phospho-p70 S6 kinase (S389) (#9205), and anti-p70 S6 kinase (#2708) were purchased from Cell Signaling Technology. pX330-U6-Chimeric_BB-CBh-hSpCas9 (pX330) was a gift from F. Zhang (Addgene plasmid #42230) (61).

cDNA microarray

Gene expression analysis was performed using a SurePrint G3 Human GE 8 × 60K microarray (Agilent) according to the manufacturer's protocol. Briefly, HCT116 $p53^{+/+}$ and HCT116 $p53^{-/-}$ cells were treated with ADR (2 µg/ml) for 2 hours and incubated at 37°C until harvest. At 0, 12, 24, and 48 hours after treatment, total RNA was isolated from the cells using standard protocols. Each RNA sample was labeled and hybridized to array slides.

Mass spectrometric analysis

HCT116 $p53^{+/+}$ or $p53^{-/-}$ cells were harvested at 0, 12, 24, 48, or 72 hours after ADR treatment. Cells were lysed in 8 M urea and 50 mM Hepes-NaOH (pH 8) and reduced with 10 mM tris(2-carboxyethyl) phosphine (Sigma) at 37°C for 30 min, followed by alkylation with 50 mM iodoacetamide (Sigma) at 25°C in the dark for 45 min. Proteins were digested with immobilized trypsin (Thermo Fisher Scientific) at 37°C for 6 hours. The resulting peptides were desalted by the Oasis HLB µElution Plate (Waters) and analyzed by LTQ Orbitrap Velos Mass Spectrometer (Thermo Fisher Scientific) combined with the UltiMate 3000 RSLCnano System (Thermo Fisher Scientific). The tandem mass spectrometry (MS/MS) spectra were searched against *Homo sapiens* protein sequence database in SwissProt using Proteome Discoverer 1.4 software (Thermo Fisher Scientific), in which a false discovery rate of 1% was set for both peptide and protein identification filters. Differential peptide quantification analysis (label-free quantification analysis) for 10 samples was performed on

Expressionist Server platform (Genedata AG), as described in a previous study (62).

Transcriptome and proteome data processing

In the transcriptome analysis, we filtered 47,534 peaks (derived from 22,276 genes) according to the following criteria for quantification of the mRNA abundance changes: (i) peak intensity at 24 hours in HCT116 $p53^{+/+}$ cells to maximum peak intensity in HCT116 $p53^{-/-}$ cells data set ratio > 2.5; (ii) in the 12-hour data set, the $\log_2$ of peak intensity at 12 hours to 0 hour ratio was >1 in HCT116 $p53^{+/+}$ cells and between −0.5 and 0.5 in HCT116 $p53^{-/-}$ cells; and (iii) in the 24- and 48-hour data sets, the $\log_2$ of peak intensity at 24 or 48 hours to 0 hour ratio was >2 in HCT116 $p53^{+/+}$ cells and between −1 and 1 in HCT116 $p53^{-/-}$ cells. As final p53 target candidates in the transcriptome analysis, genes selected with at least two different time points were extracted. In the proteome analysis, we filtered 19,004 peptides (derived from 3342 proteins) according to the following criteria for quantification of the peptide abundance changes after adding a count of one as a pseudocount: (i) peak intensity at 24 hours in HCT116 $p53^{+/+}$ cells to maximum peak intensity in HCT116 $p53^{-/-}$ cells data set ratio > 2; (ii) in the 12-hour data set, the $\log_2$ of peak intensity at 12 hours to 0 hour ratio was >1 in HCT116 $p53^{+/+}$ cells and between −0.5 and 0.5 in HCT116 $p53^{-/-}$ cells; and (iii) in the 24- and 48-hour data sets, the $\log_2$ of peak intensity at 24 or 48 hours to 0 hour ratio was >2 in HCT116 $p53^{+/+}$ cells and between −1 and 1 in HCT116 $p53^{-/-}$ cells. As final p53 target candidates in the proteome analysis, proteins selected with at least two different time points were extracted.

Mice and x-ray treatment and RNA-seq

$p53^{-/-}$ mice were provided by the RIKEN BioResource Center. Genotypes were confirmed by PCR analysis. All mice were maintained under specific pathogen–free conditions and handled in accordance with the Guidelines for Animal Experiments of the Institute of Medical Science (University of Tokyo, Tokyo, Japan). $p53^{+/+}$ and $p53^{-/-}$ mice were x-ray–irradiated using the MBR-1520R-3 System (Hitachi). At 24 hours after irradiation, 24 tissues were collected from mice. The age and gender of mice are as follows: bladder, bone marrow, cerebrum, colon, esophagus, eyeball, heart, kidney, liver, lung, muscle, seminal vesicle, small intestine, spleen, stomach, testis, thymus, and tongue: male, 6 weeks, $n = 3$ each; bone: male, 1 week, $n = 3$ each; uterus: female, 10 weeks, $n = 3$ each; mammary gland and ovary: female, 10 weeks, $n = 2$ each. Tissues were preserved in RNAlater solution (Qiagen) at 4°C until RNA purification. Bone marrow was resolved in RLT Plus reagent provided by the RNeasy Plus Mini Kit (Qiagen) and homogenized using a QIAshredder column (Qiagen). The lysates were stored at −80°C until RNA purification.

Tissues were homogenized in QIAzol lysis reagent (Qiagen) using Precellys 24 (Bertin Corporation). Total RNA was recovered using the RNeasy Plus Universal Mini Kit (Qiagen). For RNA extraction from bone marrow, we used the RNeasy Plus Mini Kit (Qiagen). We selected 256 samples for RNA-seq analysis based on RNA quality and quantity, which were evaluated using a Bioanalyzer (Agilent) and NanoDrop (Thermo Fisher Scientific). High-quality RNA was subjected to polyadenylated selection and chemical fragmentation, and a 100- to 200-base RNA fraction was used to construct complementary DNA (cDNA) libraries according to Illumina's protocol. RNA-seq was performed on a HiSeq 2500 using a standard paired-end 101–base pair (bp) protocol. We used a TopHat + Cufflinks pipeline to

process raw RNA-seq data. Before data processing, the quality of data was checked with FastQC. To quantify gene and transcript expression levels for all samples, we first aligned 101-bp paired-end reads to the mouse reference genome mm9/GRCm37 using TopHat (v2.0.9). The mapping parameters follow the default setting in the TopHat. After the read mapping, transcript and gene expression levels, which are represented by FPKM (fragments per kilobase per million) values, were calculated by Cufflinks (v2.2.1).

$Ass1^{+/-}$ mice were purchased from The Jackson Laboratory. All mice were maintained under specific pathogen–free conditions and handled in accordance with the Guidelines for Animal Experiments of the University of Tokyo. $Ass1^{+/+}$ and $Ass1^{+/-}$ mice at 8 weeks of age were irradiated with 10 Gy of x-ray irradiation. At 1 or 10 days after irradiation, mice were sacrificed. Arginine-free food (#510131) and its control food (#510025) were purchased from Clea Japan Inc.

Real-time qPCR
Total RNA was isolated from human cells using the RNeasy Plus Mini Kit (Qiagen) and RNeasy Plus Universal Mini Kit (Qiagen) according to the manufacturer's instructions. cDNAs were synthesized using SuperScript III Reverse Transcriptase (Invitrogen). Real-time qPCR was conducted using SYBR Green Master Mix on a LightCycler 480 (Roche). Primer sequences are as follows: human ASS1, 5′-AGCTCAGCTGCTACTCACTGG-3′ (forward) and 5′-TTG-AACCGGTTGTAGAATTCAG-3′ (reverse); mice Ass1, 5′-ACT-CAGGACCCTGCCAAAG-3′ (forward) and 5′-GCCATCTTT-GATGTTGGTCA-3′ (reverse); human p21/CDKN1A, 5′-GACC-TGTCACTGTCTTGTACCC-3′ (forward) and 5′-AAGATCA-GCCGGCGTTTG-3′ (reverse); human β-actin, 5′-TTCTGGCC-TGGAGGCTATC-3′ (forward) and 5′-TCAGGAAATTTGAC-TTTCCATTC-3′ (reverse); mice Gapdh, 5′-AATGTGTCCGTCG-TGGATCTGA-3′ (forward) and 5′-GATGCCTGCTTCACCA-CCTTCT-3′ (reverse).

Western blot analysis
Total cell lysates were prepared with lysis buffer containing 50 mM tris-HCl (pH 7.5), 100 mM NaCl, 1% NP-40, protease inhibitor cocktail set III (Calbiochem), and phosphatase inhibitor cocktail set II (Merck Millipore) and normalized by protein concentration using the bicinchoninic acid method (Thermo Fisher Scientific). For animal studies, freshly resected tissues frozen in liquid nitrogen were homogenized in radioimmunoprecipitation assay buffer (Thermo Fisher Scientific) containing 1 mM phenylmethylsulfonyl fluoride, 0.1 mM dithiothreitol, protease inhibitor cocktail set III (Calbiochem), and phosphatase inhibitor cocktail set II (Merck Millipore) and normalized by protein concentration using the Pierce 660 nm Protein Assay Reagent (Thermo Fisher Scientific). For Western blotting, protein samples were separated on SDS–polyacrylamide gel electrophoresis and transferred to nitrocellulose membranes (Hybond ECL, Amersham). Membranes were blocked in tris-buffered saline–Tween 20 containing 5% nonfat milk for 1 hour at room temperature. Then, the membranes were incubated with primary antibodies according to the manufacturer's instructions for 18 hours at 4°C. After that, the membranes were incubated with horseradish peroxidase (HRP)–conjugated goat anti-rabbit, goat anti-mouse, or donkey anti-goat IgG (Santa Cruz Biotechnology) and visualized by chemiluminescent detection (Immobilon, Millipore). Image quantification was performed by ImageJ (National Institutes of Health) from three independent experiments.

Plasmid construction
The potential p53 response elements (p53REs) located in intron 1 of human ASS1 were amplified and subcloned into the pGL4.24 vector (Promega). Point mutations "T" were inserted at the 4th and the 14th nucleotide "C" and the 7th and the 17th nucleotide "G" of each p53RE by site-directed mutagenesis. Primers used for these plasmid constructions are as follows: p53RE amplification, 5′-ACACCTCGAGAGG-CAGGGTCATTGTGAAAG-3′ (forward) and 5′-AGAGAGATCT-CATCACTGGGTTTGTGCTTG-3′ (reverse); mutagenesis, 5′-AGA-TCTTTTCTCTCCCCAGGGGTAGATC-3′ (forward) and 5′-GTT-ACTACCCTGAGACCTGCAGCC-3′ (reverse). All constructs were verified by sequencing after subcloning.

ChIP assay
The ChIP assay was performed using the EZ-Magna ChIP G Kit (Merck Millipore) following the manufacturer's protocol. Briefly, HCT116 $p53^{+/+}$ cells treated with ADR (2 μg/ml) and U373MG cells infected with Ad-p53 or Ad-LacZ at an MOI of 10 were cross-linked with 1% formaldehyde for 10 min, washed with phosphate-buffered saline (PBS), and lysed in nuclear lysis buffer. The lysate was then sonicated using the Bioruptor UCD-200 (Cosmo Bio) to shear DNA to approximately 200 to 1000 bp. Supernatant from 1×10^6 cells was used for each immunoprecipitation with anti-p53 antibody (OP140, Merck Millipore) or normal mouse IgG (sc-2025, Santa Cruz Biotechnology). Column-purified DNA was quantified by qPCR. Human ASS1 binding site was amplified by using the following primers: 5′-AGAGTCC-ACTCCCGAGCAG-3′ (forward) and 5′-ATCAAAGCCCAAGTCC-CCTA-3′ (reverse). Human p21/CDKN1A binding site was amplified by using the following primers: 5′-CTGGACTGGGCACTCTTGTC-3′ (forward) and 5′-CTCCTACCATCCCCTTCCTC-3′ (reverse).

Gene reporter assay
Reporter assays were performed using the Dual-Luciferase Assay System (Promega), as described previously (63).

Generation of ASS1 knockout clones using the CRISPR-Cas9 system
The CRISPR guide sequences designed to exon 3 of ASS1 or the AAVS1 locus using http://crispr.mit.edu/ were cloned into pX330 (AAVS1, GGGGCCACTAGGGACAGGAT; ASS1-1, GTGCTGGACATAG-CGTCTGGC; and ASS1-2, GACACCTCGTGCATCCTCGTG).

HCT116 cells (800,000 per dish) were plated into 6-cm dishes and cotransfected 24 hours later with 3 μg of pX330 expressing the above guide RNAs and pcDNA3 using FuGENE6. Cells were trypsinized 48 hours later. Then, G418 (0.6 mg/ml) was applied for 10 to 14 days, and cells were allowed to recover for a few days. When cells were approaching confluency, they were seeded sparsely in 10-cm dishes. A few weeks later, discernible colonies were isolated using cloning discs (Sigma). Individual clones were expanded and evaluated for knockout status by Western blot analysis for ASS1.

ASS1 activity assay
The procedure was carried out essentially as described (64). Briefly, cells treated with or without ADR and x-ray irradiation were washed with PBS and stored frozen at −80°C until use. Frozen cells were resuspended into buffer A [50 mM tris-HCl (pH 8), 10% glycerol, protease inhibitor cocktail (Calbiochem)] and then left on ice for 10 min. After centrifugation for 20 min at 15,000 rpm at 4°C, 10 μg of proteins was added to the reaction buffer [20 mM tris-HCl (pH 7.8),

2 mM adenosine 5′-triphosphate, 2 mM citrulline, 2 mM aspartate, 6 mM MgCl$_2$, 20 mM KCl, and 0.1 U pyrophosphatase] to a final volume of 0.1 ml. Samples were incubated for 60 min at 37°C. The reactions were stopped by the addition of an equal volume of molybdate buffer (10 mM ascorbic acid, 2.5 mM ammonium molybdate, and 2% sulfuric acid). Accumulation of pyrophosphate, a by-product of argininosuccinate synthesis, was determined spectrophotometrically at 660 nm.

Metabolite measurements
Amino acid concentrations in mouse plasma were measured using the LC-MS system (Oriental Yeast Co. Ltd.).

Clinical chemistry parameters test
Clinical chemistry parameters of Ass1$^{+/+}$ and Ass1$^{+/−}$ mice were measured according to the manufacturer's protocol (Oriental Yeast Co. Ltd.).

Fluorescence-activated cell sorting analysis
Cells were collected and fixed with cold 70% ethanol overnight at 4°C. Subsequently, fixed cells were treated with ribonuclease A (1 mg/ml) for 30 min at room temperature and then stained with propidium iodide (50 μg/ml). Cells were analyzed on a flow cytometer (Beckman Coulter).

Cell viability assay
For the proliferation assay and Akt inhibitor experiments, the cell numbers were evaluated by the CellTiter-Glo Luminescent Cell Viability Assay (Promega) at the indicated times. The luminescence of cell lysates was measured by an ARVO X3 plate reader (PerkinElmer) according to the manufacturer's protocol.

Histological analysis
For histological preparations, small intestine (jejunum), colon, stomach, liver, kidney, spleen, lung, and heart were collected from mice and fixed overnight in 10% formalin. Paraffin-embedded tissues were sectioned at 5 μm and stained with H&E.

TUNEL assay
The TUNEL assay was performed using a commercially available kit according to the manufacturer's protocol (Wako).

Immunohistochemistry
Paraffin sections of mouse small intestine were stained using anti-Ki67 antibody according to the manufacturer's protocol. For visualization, the sections were incubated with HRP-labeled polymer anti-rabbit (Dako) and 3,3′-diaminobenzidine (Dako) was used as a chromogen. Then, the samples were counterstained with hematoxylin.

Statistical analysis
Statistical analysis was performed using an unpaired two-tailed Student's t test. The F test was used to determine whether variances were equal or unequal. A one-way ANOVA was used for multiple group comparisons.

SUPPLEMENTARY MATERIALS
Supplementary material for this article is available at http://advances.sciencemag.org/cgi/content/full/3/5/e1603204/DC1
fig. S1. Schematics of the integrated multi-OMICS approach.
fig. S2. Examination of genotoxic stress–induced ASS1 mRNA expression.
fig. S3. ASS1 gene expression in a p53-dependent manner.
fig. S4. Verification of the identified p53 binding site in the ASS1 gene.
fig. S5. Schematic diagram of the p53-mediated amino acid metabolism.
fig. S6. Examination of genotoxic stress–induced ASS1 protein expression.
fig. S7. The Cdkn1a mRNA expression level in various mouse tissues after TBI.
fig. S8. Examination of x-ray irradiation–induced Ass1 protein expression.
fig. S9. Characterization of Ass1$^{+/+}$ and Ass1$^{+/−}$ mice.
fig. S10. Plasma arginine level in Ass1$^{+/+}$ and Ass1$^{+/−}$ mice.
fig. S11. The effect of Ass1 status and arginine diet on genotoxic stress sensitivity.
fig. S12. The effect of x-ray irradiation on tissue morphology and Ki-67 expression in Ass1$^{+/+}$ and Ass1$^{+/−}$ mice.
fig. S13. Examination of x-ray irradiation–induced Ass1 mRNA level in the small intestine.
fig. S14. The effect of ASS1 overexpression on Akt phosphorylation and genotoxic stress sensitivity.
fig. S15. Synergistic increase of Akt phosphorylation in Ass1-null MEFs.
fig. S16. The effect of ADR treatment on Akt signaling in p53$^{+/+}$ and p53$^{−/−}$ cells.
fig. S17. The effect of arginine supplementation on Akt phosphorylation and genotoxic stress sensitivity.
table S1. Transcriptome data of ADR-treated HCT116 cells.
table S2. Proteome data of ADR-treated HCT116 cells.

REFERENCES AND NOTES
1. K. T. Bieging, S. S. Mello, L. D. Attardi, Unravelling mechanisms of p53-mediated tumour suppression. Nat. Rev. Cancer 14, 359–370 (2014).
2. C. R. Berkers, O. D. K. Maddocks, E. C. Cheung, I. Mor, K. H. Vousden, Metabolic regulation by p53 family members. Cell Metab. 18, 617–633 (2013).
3. L. Jiang, N. Kon, T. Li, S.-J. Wang, T. Su, H. Hibshoosh, R. Baer, W. Gu, Ferroptosis as a p53-mediated activity during tumour suppression. Nature 520, 57–62 (2015).
4. S. Marshall, Role of insulin, adipocyte hormones, and nutrient-sensing pathways in regulating fuel metabolism and energy homeostasis: A nutritional perspective of diabetes, obesity, and cancer. Sci. STKE 2006, re7 (2006).
5. P. S. Ward, C. B. Thompson, Metabolic reprogramming: A cancer hallmark even Warburg did not anticipate. Cancer Cell 21, 297–308 (2012).
6. H. J. Müller, J. Boos, Use of L-asparaginase in childhood ALL. Crit. Rev. Oncol. Hematol. 28, 97–113 (1998).
7. O. D. K. Maddocks, C. R. Berkers, S. M. Mason, L. Zheng, K. Blyth, E. Gottlieb, K. H. Vousden, Serine starvation induces stress and p53-dependent metabolic remodelling in cancer cells. Nature 493, 542–546 (2013).
8. F. Xiao, C. Wang, H. Yin, J. Yu, S. Chen, J. Fang, F. Guo, Leucine deprivation inhibits proliferation and induces apoptosis of human breast cancer cells via fatty acid synthase. Oncotarget 7, 63679–63689 (2016).
9. M. P. Kelly, A. A. Jungbluth, B.-W. Wu, J. Bomalaski, L. J. Old, G. Ritter, Arginine deiminase PEG20 inhibits growth of small cell lung cancers lacking expression of argininosuccinate synthetase. Br. J. Cancer 106, 324–332 (2012).
10. P. A. Ascierto, S. Scala, G. Castello, A. Daponte, E. Simeone, A. Ottaiano, G. Beneduce, V. De Rosa, F. Izzo, M. T. Melucci, C. M. Ensor, A. W. Prestayko, F. W. Holtsberg, J. S. Bomalaski, M. A. Clark, N. Savaraj, L. G. Feun, T. F. Logan, Pegylated arginine deiminase treatment of patients with metastatic melanoma : Results from phase I and II studies. J. Clin. Oncol. 23, 7660–7668 (2005).
11. J. A. Mcalpine, H.-T. Lu, K. C. Wu, S. K. Knowles, J. A. Thomson, Down-regulation of argininosuccinate synthetase is associated with cisplatin resistance in hepatocellular carcinoma cell lines : Implications for PEGylated arginine deiminase combination therapy. BMC Cancer 14, 621 (2014).
12. A. Husson, C. Brasse-lagnel, A. Fairand, S. Renouf, A. Lavoinne, Argininosuccinate synthetase from the urea cycle to the citrulline–NO cycle. Eur. J. Biochem. 270, 1887–1899 (2003).
13. H.-Y. Huang, W.-R. Wu, Y.-H. Wang, J.-W. Wang, F.-M. Fang, J.-W. Tsai, S.-H. Li, H.-C. Hung, S.-C. Yu, J. Lan, Y.-L. Shiue, C.-H. Hsing, L.-T. Chen, C.-F. Li, ASS1 as a novel tumor suppressor gene in myxofibrosarcomas: Aberrant loss via epigenetic DNA methylation confers aggressive phenotypes, negative prognostic impact, and therapeutic relevance. Clin. Cancer Res. 19, 2861–2872 (2013).
14. F. Qiu, Y.-R. Chen, X. Liu, C.-Y. Chu, L.-J. Shen, J. Xu, S. Gaur, H. J. Forman, H. Zhang, S. Zheng, Y. Yen, J. Huang, H.-J. Kung, D. K. Ann, Arginine starvation impairs mitochondrial respiratory function in ASS1-deficient breast cancer cells. Sci. Signal. 7, ra31 (2014).
15. B. Delage, D. A. Fennell, L. Nicholson, I. McNeish, N. R. Lemoine, T. Crook, P. W. Szlosarek, Arginine deprivation and argininosuccinate synthetase expression in the treatment of cancer. Int. J. Cancer 126, 2762–2772 (2010).

16. C.-L. Wei, Q. Wu, V. B. Vega, K. P. Chiu, P. Ng, T. Zhang, A. Shahab, H. C. Yong, Y. T. Fu, Z. Weng, J. J. Liu, X. Dong Zhao, J.-L. Chew, Y. Ling Lee, V. A. Kuznetsov, W.-K. Sung, L. D. Miller, B. Lim, E. T. Liu, Q. Yu, H.-H. Ng, Y. Ruan, A global map of p53 transcription-factor binding sites in the human genome. *Cell* **124**, 207–219 (2006).

17. S. Suzuki, T. Tanaka, M. V. Poyurovsky, H. Nagano, T. Mayama, Y. Suzuki, S. Sugano, E. Sato, T. Nagao, K. Yokote, I. Tatsuno, C. Prives, Phospho-activated glutaminase (GLS2), a p53-inducible regulator of glutamine metabolism and reactive oxygen species. *Proc. Natl. Acad. Sci. U.S.A.* **107**, 7461–7466 (2010).

18. A. Zauberman, D. Flusberg, Y. Haupt, Y. Barak, M. Oren, A functional p53-responsive intronic promoter is contained within the human mdm2 gene. *Nucleic Acids Res.* **23**, 2584–2592 (1995).

19. C. Tanikawa, K. Ueda, H. Nakagawa, N. Yoshida, Y. Nakamura, K. Matsuda, Regulation of protein citrullination through p53/PADI4 network in DNA damage response. *Cancer Res.* **69**, 8761–8769 (2009).

20. M. A. Allen, Z. Andrysik, V. L. Dengler, H. S. Mellert, A. Guarnieri, J. A. Freeman, K. D. Sullivan, M. D. Galbraith, X. Luo, W. L. Kraus, R. D. Dowell, J. M. Espinosa, Global analysis of p53-regulated transcription identifies its direct targets and unexpected regulatory mechanisms. *eLife* **3**, e02200 (2014).

21. C. Tovar, J. Rosinski, Z. Filipovic, B. Higgins, K. Kolinsky, H. Hilton, X. Zhao, B. T. Vu, W. Qing, K. Packman, O. Myklebost, D. C. Heimbrook, L. T. Vassilev, Small-molecule MDM2 antagonists reveal aberrant p53 signaling in cancer: Implications for therapy. *Proc. Natl. Acad. Sci. U.S.A.* **103**, 1888–1893 (2006).

22. T. Riley, E. Sontag, P. Chen, A. Levine, Transcriptional control of human p53-regulated genes. *Nat. Rev. Mol. Cell Biol.* **9**, 402–412 (2008).

23. K.-A. Yoon, Y. Nakamura, H. Arakawa, Identification of *ALDH4* as a p53-inducible gene and its protective role in cellular stresses. *J. Hum. Genet.* **49**, 134–140 (2004).

24. K. Polyak, Y. Xia, J. L. Zweier, K. W. Kinzler, B. Vogelstein, A model for p53-induced apoptosis. *Nature* **389**, 300–305 (1997).

25. Y. Yu, K. Terada, A. Nagasaki, M. Takiguchi, M. Mori, Preparation of recombinant argininosuccinate synthetase and argininosuccinate lyase: Expression of the enzymes in rat tissues. *J. Biochem.* **117**, 952–957 (1995).

26. M. Morifuji, M. Ishizaka, S. Baba, K. Fukuda, H. Matsumoto, J. Koga, M. Kanegae, M. Higuchi, Comparison of different sources and degrees of hydrolysis of dietary protein: Effect on plasma amino acids, dipeptides, and insulin responses in human subjects. *J. Agric. Food Chem.* **58**, 8788–8797 (2010).

27. J. A. Hammer III, D. E. Rannelst, Protein turnover in pulmonary macrophages. Utilization of amino acids derived from protein degradation. *Biochem. J.* **198**, 53–65 (1981).

28. Y. Luo, J. Yoneda, H. Ohmori, T. Sasaki, K. Shimbo, S. Eto, Y. Kato, H. Miyano, T. Kobayashi, T. Sasahira, Y. Chihara, H. Kuniyasu, Cancer usurps skeletal muscle as an energy repository. *Cancer Res.* **74**, 330–340 (2014).

29. E. A. Komarova, R. V. Kondratov, K. Wang, K. Christov, T. V. Golovkina, J. R. Goldblum, A. V. Gudkov, Dual effect of p53 on radiation sensitivity in vivo: p53 promotes hematopoietic injury, but protects from gastro-intestinal syndrome in mice. *Oncogene* **23**, 3265–3271 (2004).

30. P. Zheng, B. Yu, J. He, G. Tian, Y. Luo, X. Mao, K. Zhang, L. Che, D. Chen, Protective effects of dietary arginine supplementation against oxidative stress in weaned piglets. *Br. J. Nutr.* **109**, 2253–2260 (2013).

31. L. Shan, B. Wang, G. Gao, W. Cao, Y. Zhang, L-Arginine supplementation improves antioxidant defenses through L-arginine/nitric oxide pathways in exercised rats. *J. Appl. Physiol.* **115**, 1146–1155 (2013).

32. F. C. M. Pinto, P. Campos-Silva, D. B. de Souza, W. S. Costa, F. J. B. Sampaio, Nutritional supplementation with arginine protects radiation-induced effects. An experimental study. *Acta Cir. Bras.* **31**, 650–654 (2016).

33. J. Shukla, J. Chatterjee, V. S. Thakur, S. Premachandran, R. Checker, T. B. Poduval, L-Arginine reverses radiation-induced immune dysfunction: The need for optimum treatment window. *Radiat. Res.* **171**, 180–187 (2009).

34. J. L. Medeiros Jr., W. S. Costa, B. Felix-Patricio, F. J. B. Sampaio, L. E. M. Cardoso, Protective effects of nutritional supplementation with arginine and glutamine on the penis of rats submitted to pelvic radiation. *Andrology* **2**, 943–950 (2014).

35. C. J. Perez, J. Jaubert, J.-L. Guénet, K. F. Barnhart, C. M. Ross-Inta, V. C. Quintanilla, I. Aubin, J. L. Brandon, N. W. Otto, J. DiGiovanni, I. Gimenez-Conti, C. Giulivi, D. F. Kusewitt, C. J. Conti, F. Benavides, Two hypomorphic alleles of mouse *Ass1* as a new animal model of citrullinemia type I and other hyperammonemic syndromes. *Am. J. Pathol.* **177**, 1958–1968 (2010).

36. K. Engel, W. Höhne, J. Häberle, Mutations and polymorphisms in the human argininosuccinate synthetase (ASS1) gene. *Hum. Mutat.* **30**, 300–307 (2009).

37. T. Miyamoto, S. Razavi, R. Derose, T. Inoue, Synthesizing biomolecule-based Boolean logic gates. *ACS Synth. Biol.* **2**, 72–82 (2013).

38. A. V. Budanov, M. Karin, p53 target genes Sestrin1 and Sestrin2 connect genotoxic stress and mTOR signaling. *Cell* **134**, 451–460 (2008).

39. X. Li, Y. Lu, K. Liang, B. Liu, Z. Fan, Differential responses to doxorubicin-induced phosphorylation and activation of Akt in human breast cancer cells. *Breast Cancer Res.* **7**, R589–R597 (2005).

40. K. G. Foster, D. C. Fingar, Mammalian target of rapamycin (mTOR): Conducting the cellular signaling. *J. Biol. Chem.* **285**, 14071–14077 (2010).

41. D. D. Sarbassov, D. A. Guertin, S. M. Ali, D. M. Sabatini, Phosphorylation and regulation of Akt/PKB by the rictor-mTOR complex. *Science* **307**, 1098–1101 (2005).

42. M. Los, S. Maddika, B. Erb, K. Schulze-Osthoff, Switching Akt: From survival signaling to deadly response. *Bioessays* **31**, 492–495 (2009).

43. C. M. Ensor, F. W. Holtsberg, J. S. Bomalaski, M. A. Clark, Pegylated arginine deiminase (ADI-SS PEG$_{20,000 \text{ mw}}$) inhibits human melanomas and hepatocellular carcinomas in vitro and in vivo. *Cancer Res.* **62**, 5443–5450 (2002).

44. B. Cao, M. Li, W. Zha, Q. Zhao, R. Gu, L. Liu, J. Shi, J. Zhou, F. Zhou, X. Wu, Z. Wu, G. Wang, J. Aa, Metabolomic approach to evaluating adriamycin pharmacodynamics and resistance in breast cancer cells. *Metabolomics* **9**, 960–973 (2013).

45. S. Wang, Z.-Y. Tsun, R. L. Wolfson, K. Shen, G. A. Wyant, M. E. Plovanich, E. D. Yuan, T. D. Jones, L. Chantranupong, W. Comb, T. Wang, L. Bar-Peled, R. Zoncu, C. Straub, C. Kim, J. Park, B. L. Sabatini, D. M. Sabatini, Lysosomal amino acid transporter SLC38A9 signals arginine sufficiency to mTORC1. *Science* **347**, 188–194 (2015).

46. M. Laplante, D. M. Sabatini, mTOR signaling in growth control and disease. *Cell* **149**, 274–293 (2012).

47. X.-d. Zhang, Z.-h. Qin, J. Wang, The role of p53 in cell metabolism. *Acta Pharmacol. Sin.* **31**, 1208–1212 (2010).

48. P. V. Hornbeck, J. M. Kornhauser, S. Tkachev, B. Zhang, E. Skrzypek, B. Murray, V. Latham, M. Sullivan, PhosphoSitePlus: A comprehensive resource for investigating the structure and function of experimentally determined post-translational modifications in man and mouse. *Nucleic Acids Res.* **40**, D261–D270 (2012).

49. W.-B. Tsai, I. Aiba, S.-y. Lee, L. Feun, N. Savaraj, M. Tien Kuo, Resistance to arginine deiminase treatment in melanoma cells is associated with induced argininosuccinate synthetase expression involving c-Myc/HIF-1α/Sp4. *Mol. Cancer Ther.* **8**, 3223–3233 (2009).

50. R. C. Blantz, J. Satriano, F. Gabbai, C. Kelly, Biological effects of arginine metabolites. *Acta Physiol. Scand.* **168**, 21–25 (2000).

51. G. Wu, F. W. Bazer, T. A. Davis, S. W. Kim, P. Li, J. Marc Rhoads, M. Carey Satterfield, S. B. Smith, T. E. Spencer, Y. Yin, Arginine metabolism and nutrition in growth, health and disease. *Amino Acids* **37**, 153–168 (2009).

52. G. Wu, S. M. Morris Jr., Arginine metabolism: Nitric oxide and beyond. *Biochem. J.* **17**, 1–17 (1998).

53. I. Vivanco, C. L. Sawyers, The phosphatidylinositol 3-kinase–AKT pathway in human cancer. *Nat. Rev. Cancer* **2**, 489–501 (2002).

54. V. Stambolic, D. MacPherson, D. Sas, Y. Lin, B. Snow, Y. Jang, S. Benchimol, T. W. Mak, Regulation of PTEN transcription by p53. *Mol. Cell* **8**, 317–325 (2001).

55. T. Kawase, R. Ohki, T. Shibata, S. Tsutsumi, N. Kamimura, J. Inazawa, T. Ohta, H. Ichikawa, H. Aburatani, F. Tashiro, Y. Taya, PH domain–only protein PHLDA3 is a p53-regulated repressor of Akt. *Cell* **136**, 535–550 (2009).

56. S. M. Bode-Böger, F. Scalera, L. J. Ignarro, The L-arginine paradox: Importance of the L-arginine/asymmetrical dimethylarginine ratio. *Pharmacol. Ther.* **114**, 295–306 (2007).

57. X. Gao, J. Zhang, Spatiotemporal analysis of differential Akt regulation in plasma membrane microdomains. *Mol. Biol. Cell* **19**, 4366–4373 (2008).

58. H. Miura, M. Matsuda, K. Aoki, Development of a FRET biosensor with high specificity for Akt. *Cell Struct. Funct.* **39**, 9–20 (2014).

59. A. Synakiewicz, T. Stachowicz-Stencel, E. Adamkiewicz-Drozynska, The role of arginine and the modified arginine deiminase enzyme ADI-PEG 20 in cancer therapy with special emphasis on Phase I/II clinical trials. *Expert Opin. Invest. Drugs* **23**, 1517–1529 (2014).

60. K. Oda, H. Arakawa, T. Tanaka, K. Matsuda, C. Tanikawa, T. Mori, H. Nishimori, K. Tamai, T. Tokino, Y. Nakamura, Y. Taya, p53AIP1, a potential mediator of p53-dependent apoptosis, and its regulation by Ser-46-phosphorylated p53. *Cell* **102**, 849–862 (2000).

61. L. Cong, F. A. Ran, D. Cox, S. Lin, R. Barretto, N. Habib, P. D. Hsu, X. Wu, W. Jiang, L. A. Marraffini, F. Zhang, Multiplex genome engineering using CRISPR/Cas systems. *Science* **339**, 819–823 (2013).

62. K. Ueda, N. Ishikawa, A. Tatsuguchi, N. Saichi, R. Fujii, H. Nakagawa, Antibody-coupled monolithic silica microtips for highthroughput molecular profiling of circulating exosomes. *Sci. Rep.* **4**, 6232 (2014).

63. C. Tanikawa, K. Matsuda, S. Fukuda, Y. Nakamura, H. Arakawa, p53RDL1 regulates p53-dependent apoptosis. *Nat. Cell Biol.* **5**, 216–223 (2003).

64. J. R. Guerreiro, C. Lameu, E. F. Oliveira, C. F. Klitzke, R. L. Melo, E. Linares, O. Augusto, J. W. Fox, I. Lebrun, S. M. T. Serrano, A. C. M. Camargo, Argininosuccinate synthetase is a functional target for a snake venom anti-hypertensive peptide: Role in arginine and nitric oxide production. *J. Biol. Chem.* **284**, 20022–20033 (2009).